

Four-fermion interactions and emergent symmetry in a non-Fermi liquid

Rokas Veitas

An essay submitted
for partial fulfillment of
Perimeter Scholars International

June, 2023

Contents

1	Introduction	2
2	The hot-spot theory	3
2.1	The bare hot-spot action	4
2.2	Renormalizing the hot-spot theory	7
2.3	Interpretation of the hot-spot theory	11
3	The full Fermi surface	12
3.1	The full action	13
3.2	Renormalizing the full theory	14
3.3	The non-Fermi liquid fixed point	16
4	The four-fermion coupling	18
4.1	Quantum corrections and beta functionals	19
4.2	The quasi-fixed point	22
5	IR symmetry group	26
5.1	Ersatz Fermi liquids	26
5.2	Emergent symmetry (or lack thereof)	28
6	Discussion	30
7	Acknowledgements	31
	References	32

Four-fermion interactions and emergent symmetry in a non-Fermi liquid

Rokas Veitas

Supervisor: Sung-Sik Lee

Non-Fermi liquids break many commonly-held intuitions surrounding metallic systems that were developed to understand the more familiar Fermi liquids. The degree to which these systems diverge from the Fermi liquid paradigm is not yet known, partially because they are usually described by strongly-interacting field theories that make computations difficult. We examine effective four-fermion interactions in one model of a non-Fermi liquid at an RG quasi-fixed point. These are irrelevant by power counting, but they are enhanced by the finite extent of the Fermi surface. We compute the quasi-fixed-point form of the four-fermion coupling in the particle-particle channel and show that it prevents the emergence of the full symmetry of the Fermi liquid.

Statement of original research

Chapter 2 primarily follows [1] and parts of [2, 3] with background notions from [4] and [5]. Chapter 3 is a review of §§IV and V of [6] and states the main results of that reference's §§VI and VII. Section 4.1 follows §VII of [6]. Section 4.2 and Chapter 5 are original research, extending [6] and connecting it with [7].

1 Introduction

The Landau Fermi liquid theory is a key pillar of condensed matter theory. First intuited by Landau to describe weakly-interacting fermions [8], it was reformulated into modern terms by Kadanoff and Wilson’s renormalization group [5, 9]. A large class of metals are very well understood from a Fermi liquid description; in spite of its gaplessness, the Fermi liquid state is quite stable to most weak perturbations from electron-electron and electron-lattice interactions (with the noteworthy exception of the BCS superconducting instability). These interactions renormalize the effective parameters of the theory, such as the mass and small-angle scattering amplitude, but do not destroy the coherence of Landau quasiparticles at low energies. In the 1970s and ’80s, experimentalists began to observe many gapless fermionic systems that are not described well by the Fermi liquid picture, including cuprates, iron pnictides, and heavy fermion compounds [10]. These systems are typically at quantum critical points, where the interaction of electrons near the Fermi surface with massless bosons that describe critical fluctuations of the order parameter of a quantum phase transition invalidates the quasiparticle paradigm. The gaplessness of these bosons makes it much more difficult to tame quantum fluctuations at low energies.

While much progress has been made in recent years in the categorization of gapped phases of matter [11–13], we are still far from a complete understanding of the wide array of gapless phases. Gapless systems are more difficult to work with because their quantum fluctuations persist to arbitrarily low energy scale, so the general problem is essentially that of solving a strongly-coupled field theory. We have far fewer models in this class that we are able to solve, even approximately, and it is therefore difficult to gain intuition on their general properties.

The model that I study in this work hinges on recent progress made in [1, 2] in solving a strongly-interacting non-Fermi liquid. In a particular model of a non-Fermi liquid arising from antiferromagnetic quantum critical fluctuations, a small parameter distinct from the coupling dynamically emerges and can be used to control the complete diagrammatic Dyson series—this enables a truly non-perturbative understanding of the theory. This gives us a concrete handhold with which to study non-Fermi liquids and a proving ground to see where and how the classic Fermi liquid theory can break down.

The model considered in [1] is called the hot-spot theory. It is very minimal, in that it assumes that the Fermi liquid description is accurate for almost all points of the Fermi surface. The validity of this assumption is examined in [6], which develops a field theory of the entire Fermi surface. This presents many challenges both conceptually and computationally. Instead of a finite number of discrete coupling constants, the theory is defined by a function's worth of information, as each coupling can take a different value at each point on the Fermi surface. The first goal of this work is to extend this program, deriving the functional form of the four-fermion coupling λ near the infrared fixed point. The second goal is to begin to characterize the low-energy emergent symmetry group of this system—the Fermi liquid has a very large symmetry group because quasiparticles at different points on the Fermi surface are conserved independently, and we show that the enhanced four-fermion interactions prevent this conservation from emerging in full.

Chapter 2 reviews the hot-spot theory of [1, 2], where we see the emergence of the nesting angle v as a small parameter that can control the Schwinger-Dyson expansion. In Chapter 3 we review the main points of the functional renormalization group formalism and we motivate and state the results obtained in [6] for the coupling functions at the non-Fermi liquid fixed point. In Chapter 4, we derive the four-point coupling function that describes the pairing interaction, which is the channel with the biggest IR divergence and thus that modifies the hot-spot theory the most. In Chapter 5, we look at the effect of this coupling function on the symmetry of the low-energy theory, and we show that the symmetry group of our non-Fermi liquid is different from that of the Fermi liquid. This provides a counterexample to a conjecture in [7] that all non-Fermi liquids have the same kinematic properties as Fermi liquids.

2 The hot-spot theory

The basis for this work is the hot-spot theory of [1]. We will describe this theory and state the results of the analysis of that paper, performing a few of the renormalization calculations to demonstrate the essence of the argument.

2.1 The bare hot-spot action

The hot-spot theory describes a $(2 + 1)$ -dimensional quantum critical point on the phase transition between a Landau Fermi liquid and a state with antiferromagnetic spin-density wave (SDW) order. The electron kinetic term of the action is given by

$$S_\psi = \sum_{\sigma=1}^{N_c} \int d\mathbf{k} \psi_\sigma^\dagger(\mathbf{k}) [ik_0 + e(\vec{k})] \psi_\sigma(\mathbf{k}). \quad (2.1)$$

Here our measure is $d\mathbf{k} = \frac{dk_0 d^2\vec{k}}{(2\pi)^3}$ and N_c is the number of spin components of ψ , which is two for an electron but we don't fix for generality. The zeroth component of $\mathbf{k} = (k_0, \vec{k})$ is a Matsubara frequency, which plays the role of an energy in condensed matter field theory calculations and is integrated over the real line for zero-temperature systems, and the vector \vec{k} is a two-dimensional spatial crystal momentum. The energy $e(\vec{k})$ is the electron dispersion, where the locus of \vec{k} such that $e(\vec{k}) = 0$ defines the Fermi surface. The dispersion that we will use is symmetric under the cyclic group of order four (C_4) and its Fermi surface is shown in Fig. 1. We will often refer to the electron as the “fermion.” This action by itself describes a Landau Fermi liquid, which arises after renormalization of a UV theory with weakly-interacting fermions. This UV history of the theory is hidden in the functional form of $e(\vec{k})$.

Spin-density wave order is defined by the order parameter

$$\Phi_\alpha(\mathbf{q}) = \int d\mathbf{k} \langle \psi_a^\dagger(\mathbf{k} + \mathbf{q}) \sigma_\alpha^{ab} \psi_b(\mathbf{k}) \rangle, \quad (2.2)$$

where the integral is taken over the Brillouin zone, σ_α are the generators of $SU(N_c)$, and $\psi_a^\dagger(\mathbf{q})$ creates a fermion with spin component a and momentum \mathbf{q} . We will also write $\Phi(\mathbf{q}) = \Phi_\alpha(\mathbf{q})\sigma^\alpha$, which is a matrix in spin space. We will often refer to this field as the “boson,” in contrast with the fermionic electron field, and it transforms in the adjoint representation of $SU(N_c)$. An SDW state will have a particular ordering vector \vec{Q} for which $\Phi((0, \vec{Q}))$ takes a nonzero value in the SDW phase. In our coordinates, antiferromagnetic order in particular is SDW order with $\vec{Q} = (\sqrt{2}\pi, 0)$, where the momentum units are such that the square Brillouin zone has width 2π .

In field-theoretic language, this is encoded in the action as the boson kinetic term,

$$S_\Phi = \frac{1}{4} \int d\mathbf{q} (q_0^2 + c_0^2 |\vec{q} - \vec{Q}|^2) \text{Tr}[\Phi(\mathbf{q})\Phi(-\mathbf{q})], \quad (2.3)$$

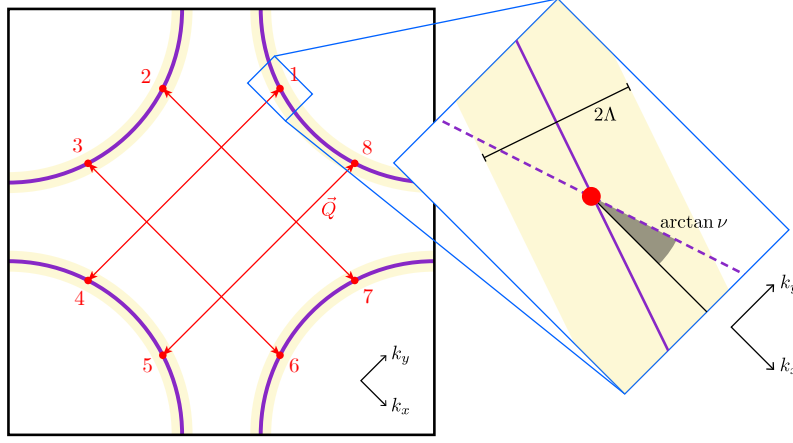


Figure 1: This purple line is a diagram of the Fermi surface of our model, defined by $e(\vec{k}) = 0$. The inside, non-simply-connected region is the hole sea, and the pieces at the corners are the electron sea. The black box defines the periodic Brillouin zone, which has width and height 2π . The hot spots, indexed by the red numbers N , are the only points on the Fermi surface connected by the SDW ordering vector \vec{Q} . The blue inset shows the linearized Fermi surface, and the dotted purple line is the “shadow Fermi surface,” the locus of momenta of electrons that start on the Fermi surface around hot spot 4 and absorb a boson of momentum \vec{Q} . The slope v relates the original and shadow Fermi surfaces and is called the *nesting angle*.

where c_0 is interpreted as the bare velocity of the boson, as it relates the \vec{q} with the frequency q_0 . This action is simply the first two terms in a gradient expansion of a vector field $\Phi_\alpha(\mathbf{q})$ around the distinguished point $(0, \vec{Q})$.

Next, we minimally couple the fermion and the boson in order to get an interacting theory. The minimal coupling between a fermion and a boson that respects both the $SU(N_c)$ symmetry that we have imposed and lattice translational symmetry is the Yukawa term

$$S_{\psi\Phi} = g \int d\mathbf{k} d\mathbf{q} \Phi^\alpha(\mathbf{q}) \psi_a^\dagger(\mathbf{k}) \sigma_\alpha^{ab} \psi_b(\mathbf{k} + \mathbf{q}), \quad (2.4)$$

where g is a coupling constant. The conservation of crystal momentum is a consequence of lattice translational symmetry. The total theory is $S = S_\psi + S_\Phi + S_{\psi\Phi}$.

We are interested in the low-energy limit of this theory. For the fermions, an energy cutoff Λ restricts our path integrals to lie only in a shell of width 2Λ around the Fermi surface. For the bosons, it keeps us to $|\vec{q} - \vec{Q}|^2 < \Lambda/c_0^2$.

This means that the interaction term will only be able to apply to pairs of fermions that are both on or near the Fermi surface and (approximately) connected by the vector \vec{Q} , which is $(\pm\sqrt{2}\pi, 0)$ or $(0, \pm\sqrt{2}\pi)$ up to Brillouin-zone periodicity. For the Fermi surfaces with C_4 symmetry like ours, there are generically eight *hot spots* which fulfill both of these criteria at arbitrarily small cutoff. Fermions away from the hot spots only enter the action through the kinetic term, so their low-energy theory is simply that of a Fermi liquid, where every point on the Fermi surface is entirely decoupled. The fermions at the hot spots need to be considered separately. A minimal theory that only includes the non-free degrees of freedom can thus be written as

$$\begin{aligned}
S = & \sum_{N=1}^8 \sum_{\sigma=1}^{N_c} \int d\mathbf{k} \psi_{N,\sigma}^\dagger(\mathbf{k}) \left[i k_0 + e_N(\vec{k}; v) \right] \psi_{N,\sigma}(\mathbf{k}) \\
& + \frac{1}{4} \int d\mathbf{q} \left(q_0^2 + c_0^2 |\vec{q}|^2 \right) \text{Tr}[\Phi(\mathbf{q})\Phi(-\mathbf{q})] \\
& + g \sum_{N=1}^8 \sum_{\sigma,\sigma'=1}^{N_c} \int d\mathbf{k} d\mathbf{q} \Phi^\alpha(\mathbf{q}) \psi_{N,\sigma'}^\dagger(\mathbf{k} + \mathbf{q}) \sigma_\alpha^{\sigma,\sigma'} \psi_{\bar{N},\sigma}(\mathbf{k}), \quad (2.5)
\end{aligned}$$

where N is a hot spot index as appears in Fig. 1, and we've shifted the definitions of the fields as functions of \mathbf{k} and \mathbf{q} such that the fermion momenta are measured from the hot spots and the boson momenta are measured from the ordering vector \vec{Q} . The notation \bar{N} refers to the hot spot connected to N via \vec{Q} ; e.g., $\bar{1} = 4$, $\bar{2} = 7$, etc. We only need to know the fermion dispersions very close to the hot spots, so we expand and drop all but linear terms:

$$\begin{aligned}
e_1(\vec{k}, v) &= -e_5(\vec{k}, v) = v k_x + k_y \\
e_4(\vec{k}, v) &= -e_8(\vec{k}, v) = v k_x - k_y,
\end{aligned}$$

and the dispersions for $N = 2, 3, 6, 7$ can be obtained from $\pi/2$ rotations of these, interchanging k_x and k_y . The parameter v is called the *nesting angle*: when two finite-measure pieces of the Fermi surface are connected by an ordering vector like \vec{Q} , they are said to be “nested,” and the nesting angle v describes the degree to which our system is not nested. It is the same at all hot spots because of C_4 symmetry. We primarily will care about the limit when v is much less than unity, so for hot spots 1, 4, 5, and 8, we will refer to k_x as the direction *along* the Fermi surface and k_y as the direction *perpendicular* to the Fermi surface, and for the other hotspots the names are flipped. Because it is a real parameter of our theory, we will call v a coupling, on equal footing with g , and we will see that it runs under RG flow.

2.2 Renormalizing the hot-spot theory

The scaling transformation in the usual prescription for renormalization of QFTs would declare the kinetic terms for the boson and the fermion as marginal, allowing the coupling constant to run. We call this Gaussian scaling, as it flows our system to the non-interacting Gaussian fixed point in the absence of a four-boson interaction. Under Gaussian scaling, our fields have tree-level scalings $[\psi] = -2$, $[\Phi] = -5/2$, and the Yukawa coupling has dimension $[g] = 1/2$, which means that it is irrelevant. In a low-dimensional system like ours, however, the quantum corrections to dimension of the coupling under Gaussian scaling can be large at low energy [14].

In order to account for the effects of the coupling from the very beginning, we use the “interaction-driven scaling,” originally proposed for a different model in [15], which has $[\psi] = [\Phi] = -2$, $[g] = 0$. This is initially an ansatz, but it can be verified *post facto* by computing the anomalous scaling dimensions of the fields. This scaling scales the bare kinetic term of the boson to zero, which naïvely would mean that the theory is singular and useless. However, under renormalization from the now-marginal interaction term, the boson acquires a new, renormalized propagator, deriving entirely from the interaction with hot fermions. In general, we would expect computing this propagator precisely to be unattainable beyond a few loops, as is the norm for perturbative field theory calculations. In the limit that the nesting angle v is small, however, we are able to compute this propagator exactly, renormalized by the fermions to all orders. The fully-renormalized boson propagator is

$$D(q)^{-1} = |q_0| + c(v)[|q_x| + |q_y|], \quad (2.6)$$

with $c(v) = \frac{1}{4}\sqrt{v \log(1/v)}$ an emergent “velocity.” Additionally, the coupling g flows from its UV value to a universal relation with v , given by $g = \sqrt{\pi v/2}$. We take these facts as another ansatz, and we can see that it is the correct propagator by showing that it solves the Schwinger-Dyson equation,

$$D(q)^{-1} = m_{\text{CT}} - \pi v \delta_{\alpha\beta} \sum_{N=1}^8 \int dk \text{Tr} \sigma^\alpha G_{\bar{N}}(k+q) \Gamma^\beta(k, q) G_N(k), \quad (2.7)$$

where G_N is the fully-dressed fermion propagator, $\Gamma^\beta(k, q)$ is the fully-dressed vertex function, α and β are $\text{SU}(N_c)$ indices, and m_{CT} is a mass counterterm that keeps the boson massless and projects the RG flow onto our critical point.

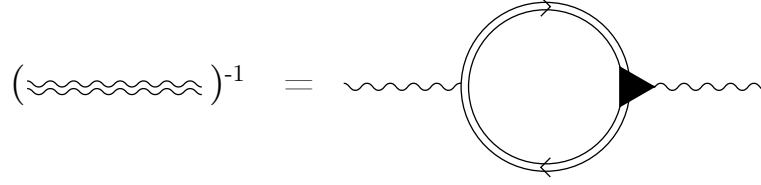


Figure 2: This is the diagrammatic form of Eq. 2.7, where the double arrowed lines are fully-dressed fermion propagators, the double wiggly line is the fully-dressed boson propagator, and the solid triangle is the fully-dressed vertex function. This can be solved exactly for small v .

There are many diagrams that contribute to Eq. 2.7 in a perturbative expansion, and we would like to estimate the magnitude of their contributions. For each fermion loop in our diagram, the integration along the Fermi surface is unbounded with perfect nesting ($v = 0$), but becomes cut off at finite v with a factor of $1/v$. All other loops have at least one boson propagator, so they have a lower cutoff of $1/c$. Because of the relationship between g and v , each vertex contributes $v^{1/2}$. Also using the graph-theory relationship $V = 2L + E - 2$, we see that

$$I \sim v^{-L_f} c^{-(L-L_f)} v^{V/2} = v^{(E-2)/2} \left(\frac{v}{c}\right)^{L-L_f}, \quad (2.8)$$

where L is the total number of loops, L_f is the number of fermion loops, E is the number of external legs, and V is the number of interaction vertices. This extra suppression of diagrams without the maximum number of fermion loops gives us a way to organize these diagrams for low v . The leading term of the Schwinger-Dyson series is the only one-loop diagram shown in Fig. 3(a), whose contribution to the self-energy is

$$\begin{aligned} \Pi^{1L}(q) &= -2\pi v \int dk \frac{1}{(i(k_0 + q_0) + vk_x + k_y + q_x + vq_y)(ik_0 + vk_x - k_y)} \\ &= -2\pi i v \int \frac{dk_0 dk_x}{(2\pi)^2} \frac{\Theta(k_0(k_0 + q_0))}{i(2k_0 + q_0) + 2vk_x + q_x + vq_y} \\ &= -2\pi \int \frac{dk_0}{2\pi} \Theta(k_0(k_0 + q_0)) \cdot \text{sgn}(2k_0 + q_0) \\ &= |q_0|. \end{aligned}$$

The spatial integrals are done by residues and the frequency integral is done

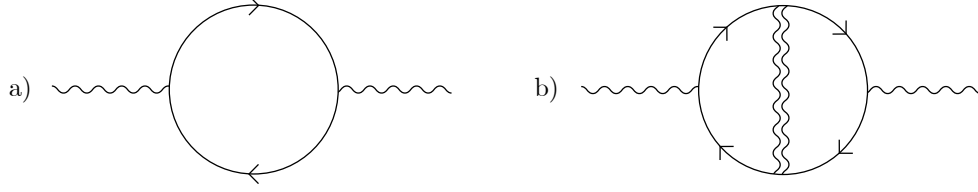


Figure 3: These are the two contributions to the Schwinger-Dyson expansion that we consider. These two diagrams, including the fully-dressed boson propagator in (b), contain the entire Schwinger-Dyson series in the low- v limit.

on the region $(-\Lambda, \Lambda)$. This doesn't have a dependence on spatial momenta and is thus unable to cut off diagrams that it contributes to, so we'd like to include one more order of v , which amounts to one more loop. The diagram of this process is shown in Fig. 3(b), and its contribution to the self-energy is

$$\begin{aligned}
 \Pi^{2L}(q) &= -\frac{\pi^2 v^2}{2} \sum_{N=1}^8 \sum_{\alpha, \beta}^2 \int dp dk \operatorname{Tr} \left[\sigma^\alpha G_N(k+p) \sigma^\beta G_{\bar{N}}(p+q+k) \sigma^\alpha G_N(q+k) \sigma^\beta G_{\bar{N}}(k) \right] D(p) \\
 &= -\frac{\pi v}{4} \sum_{N=1}^8 \int dp dk \frac{D(p)}{\left(i(k_0 + p_0) + e_N(\vec{k} + \vec{p}) \right) \left(i(q_0 + k_0) + e_N(\vec{q} + \vec{k}) \right)} \\
 &\quad \times \frac{1}{\left(i(p_0 + q_0 + k_0) + e_{\bar{N}}(\vec{p} + \vec{q} + \vec{k}) \right) \left(i k_0 + e_{\bar{N}}(\vec{k}) \right)} \\
 &= \pi^2 v^2 \sum_{N=1}^8 \int dp \frac{|p_0| - |q_0|}{\left(i(p_0 + q_0) + e_{\bar{N}}(\vec{p} + \vec{q}) \right) \left(i(p_0 - q_0) + e_N(\vec{p} - \vec{q}) \right)} D(p).
 \end{aligned}$$

We already know the $|q_0|$ dependence of $D(q)$ from the diagram of Fig. 3(a), so we can set q_0 to zero here, as anything we calculate in this diagram is bound to be at least first order in v and should be neglected in comparison with $|q_0|$. The mass term subtracts off linear divergences, so we really should be working with $\Delta \Pi^{2L}(0, \vec{q}) = \Pi^{2L}(0, \vec{q}) - \Pi^{2L}(0, 0)$. This is

$$\Delta \Pi^{2L}(0, \vec{q}) = \frac{\pi v}{8} \sum_{N=1}^8 \int dp \frac{|p_0| \mathcal{F}_N^{1L}(p_0, \vec{p}, \vec{q}; v) D(p)}{[p_0^2 + e_N^2(\vec{p} + \vec{q})][p_0^2 + e_N^2(\vec{p} - \vec{q})][p_0^2 + e_N^2(\vec{p})][p_0^2 + e_N^2(\vec{q})]}, \quad (2.9)$$

where

$$\begin{aligned} \mathcal{F}_N^{1L}(p_0, \vec{p}, \vec{q}; v) = & [p_0^2 + e_N^2(\vec{p})][p_0^2 + e_N^2(\vec{p})][ip_0 - e_N(\vec{p} + \vec{q})][ip_0 - e_N(\vec{p} - \vec{q})] \\ & - [ip_0 - e_N(\vec{p})][ip_0 - e_N(\vec{p})][p_0^2 + e_N^2(\vec{p} + \vec{q})][p_0^2 + e_N^2(\vec{p} - \vec{q})]. \end{aligned}$$

Now we will focus on hot spot 1 in order to perform this integration, recalling that $D(q)^{-1} = |q_0| + c(|q_x| + |q_y|)$, $e_1(\vec{q}) = vq_x + q_y$, and $e_4(\vec{q}) = vq_x - q_y$. At lowest order in v , all contributions from q_x are less important than those from q_y , so we drop all instances of q_x . We can also safely drop p_y inside of $D(p)$ when c is small, because the fermion dispersions in the denominator suppress high p_y . These two things simplify the situation considerably. We will rescale the momentum by $(p_0, p_x, p_y) \mapsto |q_y|(p_0, p_x/c, p_y)$; taking the p_y integral gives us

$$\Delta\Pi_{N=1}^{2L}(0, \vec{q}) = \frac{\pi v}{32\pi c} \int dp_0 dp_x \frac{(1 + p_0^2 - 3p_x^2 w^2)p_0^2}{(p_0^2 + w^2 p_x^2)[p_0^2 + (wp_x - 1)^2][p_0^2 + (wp - x + q)^2]} \frac{1}{|p_0| + |p_x|}, \quad (2.10)$$

where we've defined the small parameter $w = v/c$. The integral diverges if $w = 0$, so we can expand in small w to give

$$\Delta\Pi_{N=1}^{2L}(0, \vec{q}) = \frac{v}{32\pi c} |q_y| \int dp_0 \frac{1}{1 + p_0^2} \left[-2 \log w - 2p_0 \cot^{-1} p_0 + p_0^2 \log \frac{p_0^2}{1 + p_0^2} + O(w) \right]. \quad (2.11)$$

The final p_0 integral gives

$$\Delta\Pi_{N=1}^{2L}(0, \vec{q}) = \frac{|q_y|v}{16c} \left[\log \frac{1}{w} - 1 + O(w) \right]. \quad (2.12)$$

For small w , we only need the first term. Hot spots 1, 4, 5, and 8 all contribute identical terms, and the other four contribute terms with $|q_x|$ instead of $|q_y|$. This means that the total two-loop self-energy is

$$\Delta\Pi^{2L}(0, \vec{q}) = \frac{v}{8c} \log \left(\frac{c}{v} \right) (|q_x| + |q_y|) + O\left(\frac{v}{c}\right). \quad (2.13)$$

This almost agrees with the spatial part of our ansatz in Eq. 2.6, and the Schwinger-Dyson equation, Eq. 2.7 reduces to

$$c = \frac{v}{8c} \log \frac{c}{v}, \quad (2.14)$$

which is solved precisely for $c(v) = \frac{1}{4}\sqrt{v \log(1/v)}$ up to factors of $\log \log(1/v)$.

This all shows that the boson propagator, calculated to all orders in perturbation theory and to lowest order in v , is given by Eq. 2.6. In order to establish full self-consistency of this model, our next step would be to calculate the fermion self-energy and thence the beta function for v . This is done in App. C of [1], and it is found that

$$\frac{\partial v}{\partial \ell} = -\frac{6}{\pi^2} v^2 \log \left[4(v \log 1/v)^{-1/2} \right] = \frac{3}{\pi^2} v^2 \log v + O(\log \log 1/v), \quad (2.15)$$

whose solution goes to zero as

$$v(\ell) = \frac{\pi^2}{3} \frac{1}{\ell \log \ell}. \quad (2.16)$$

for $\ell \gg 1/v_0 \log 1/v_0$, with v_0 the initial nesting angle of the UV theory. This shows that we are justified to consider systems with small v , as theories with finite v will eventually flow there.

The other loose end of our presentation so far is the beta function for the coupling g . The fixed point at $g^2 \sim v$, was established in [2, 3] via dimensional regularization before the small- v expansion was formalized as presented here in [1]. A plot of the RG flow for a similar system with an irrelevant four-boson coupling can be seen in Fig. 4.

2.3 Interpretation of the hot-spot theory

A macroscopic way to see that the the hot-spot theory is really fundamentally different from the Fermi liquid is to measure its heat capacity. this is calculated in §IV of [1] to be

$$c_V \sim \tilde{\Lambda} T e^{2\sqrt{3} \log(1/T)^{1/2} / \log \log(1/T)}, \quad (2.17)$$

which diverges strongly from the Fermi liquid case. This comes primarily from the boson, and dominates the $c \sim k_F T$ contribution from the cold electrons away from the hot spots. The superlogarithmic correction is part of the low-energy universal data for the theory.

An unusual thing about this low-energy theory is that it isn't a true fixed point of the RG flow when considered in (v, g) coupling space: there is no positive value of v such that $\frac{\partial v}{\partial \ell} = 0$. However, g^2/v *does* flow to a fixed value of $\pi/2$ even as v and g flow to zero, so we can justify calling it the *strange*

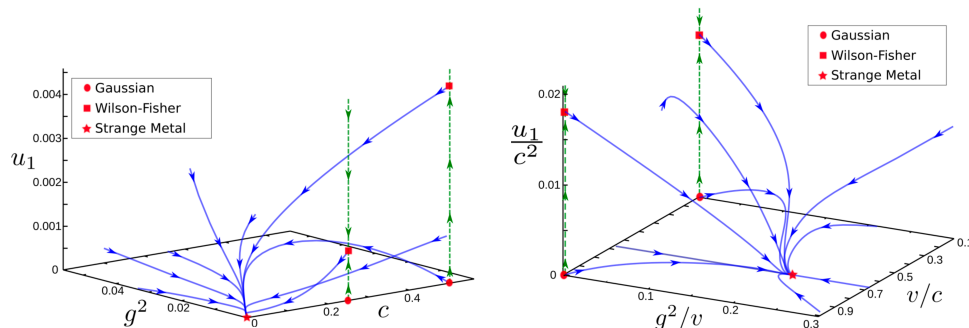


Figure 4: Here we see the RG flow calculated at one loop for the hot-spot strange metal system, using dimensional regularization from the upper critical dimension $d = 3 - \epsilon$ with $\epsilon = 0.01$. Our version doesn't include u_1 , which is a four-boson interaction that is irrelevant when g is nonzero. The couplings g and c both flow to zero, but they do so while approaching fixed ratios with v , so the strange metal fixed point is distinct from the trivial Gaussian one. This figure is reproduced from Fig. 4 of [2].

metal fixed point, distinct from the Gaussian fixed point at $g = 0$ and with its own consistently-described low-energy universal data and experimental signatures. This viewpoint is further supported by the fact that v flows very slowly to zero, as described by Eq. 2.16. This means that the strange metal with small v can be expected to describe the physics well for very long RG time. Fig. 4 shows the RG flow of this system as calculated in [2]. Note that the term “strange metal” is defined by a particular relation between temperature and resistivity that is appropriate for the hot-spot theory, but throughout the rest of this essay we will speak more generally of *non-Fermi liquids*.

3 The full Fermi surface

The hot spot theory is powerful and unusual in that it describes a strongly-interacting RG fixed point of a theory with a Fermi surface in a limit that still allows us to do calculations. However, its basic assumption, that fermions away from the hot spots are not important to the low-energy physics, can be questioned. On the level of the parameters of the original hot-spot model, it's conceivable that the couplings g and v could acquire smeared profiles in

momentum space around the hot spots, and it's worthwhile to understand what these profiles look like. More crucially, though, we have to consider several-fermion interactions.

A $2n$ -fermion coupling in dimension $d + 1$ has dimension $[\lambda^{(2n)}] = d - nd + 1$. In $2 + 1$ dimensions, this means that the four-fermion coupling has dimension $[\lambda] = -1$. In systems without Fermi surfaces, this means that as we go towards the IR, the coupling must go as $\lambda \sim \mu$ on purely dimensional grounds. When we *do* have a Fermi surface, we introduce an extra dimensionful scale k_F that defines the size of the Fermi surface and remains observable all the way into the IR. Because our quantum corrections can contain integrals over finite-dimensional submanifolds of momentum space, the low-energy coupling can be enhanced to $\lambda \sim \mu^{1-\gamma} k_F^\gamma$, where $\gamma > 0$. This motivates the inclusion of four-fermion interactions in our effective theory, but we have to actually calculate the quantum corrections to find the actual value of the exponent γ .

We don't include higher-than-four-fermion interactions in this work, and it is argued in [6] that they should not attain the maximum possible enhancement discussed in the previous paragraph and that they are thus irrelevant. However, it is still possible that they could impact the low-energy symmetry group as studied in Chapter 5, and the symmetry that remains after consider six- and higher-fermion couplings is an outstanding question.

3.1 The full action

In order to study the full Fermi surface, we must use the functional RG formalism. To capture the full low-energy theory in all generality, we have to keep track of the couplings as continuous functions of the momentum coordinate along the Fermi surface. The action for this theory is

$$\begin{aligned}
 S = & \sum_{N=1}^8 \sum_{\sigma=1}^{N_c} \int d\mathbf{k} \psi_{N\sigma}^\dagger(\mathbf{k}) \left(i k_0 + V_k^{(N)} e_N[\vec{k}, v_k^{(N)}] \right) \psi_{N\sigma}(\mathbf{k}) \\
 & + \sum_{N=1}^8 \sum_{\sigma\sigma'}^{N_c} \int d\mathbf{k} d\mathbf{q} g_{k+q,q}^{(N)} \psi_{N\sigma'}^\dagger(\mathbf{k} + \mathbf{q}) \Phi_\alpha(\mathbf{q}) \sigma_{\sigma\sigma'}^\alpha \psi_{N\sigma}(\mathbf{k}) \\
 & + \frac{1}{4\mu} \sum_{\{N_i\}}^8 \sum_{\{\sigma_i\}}^{N_c} \int \prod_{i=1}^4 d\mathbf{k}_i \delta_{1+2,3+4} \lambda_{\{k_i\}}^{\{N_i\};\{\sigma_i\}} \psi_1^\dagger(\mathbf{k}_1) \psi_2^\dagger(\mathbf{k}_2) \psi_3(\mathbf{k}_3) \psi_4(\mathbf{k}_4),
 \end{aligned} \tag{3.1}$$

where $\psi_i(\mathbf{k}_i) = \psi_{N_i\sigma_i}(\mathbf{k}_i)$. This action is an extended version of Eq. 2.5 with the same conventions. The principal difference is that we now have the

coupling functions for the Fermi velocity $V_k^{(N)}$, and the nesting angle $v_k^{(N)}$, the Yukawa coupling $g_{k+q,q}^{(N)}$, so that the theory is defined not only at the hot spots, but in eight extended patches of size $\sim k_F$ around each hot spot. We've also added the four-fermion coupling λ , normalized by the floating energy scale μ so that it doesn't scale at tree level under the interaction-driven scaling. The momentum-conserving delta functions are defined on the pattern of $\delta_{m,n} = (2\pi)^3 \delta(\mathbf{k}_m - \mathbf{k}_n)$. Boldface $\mathbf{k} = (k_0, \vec{k})$ has a Matsubara frequency as its zeroth component and a spatial momentum as the others. In isolation, the symbol k represents the component of \vec{k} along the Fermi surface, depending on the hot spot being considered: it's important to note that the coupling functions depend only on this component. Under C_4 symmetry, the coupling functions at different patches should be related to each other by

$$(v_k^{(N)}, V_k^{(N)}, g_{k',k}^{(N)}) = \begin{cases} (v_k, V_k, g_{k,k'}) & N = 1, 3, 4, 6 \\ (v_{-k}, V_{-k}, g_{-k,-k'}) & N = 2, 5, 7, 8 \end{cases}. \quad (3.2)$$

We have the freedom to set the relative scale between momentum and frequency and also to set the normalization of the boson field to fix

$$V_0 = 1, \quad g_{0,0} = \sqrt{\frac{\pi v_0}{2}}. \quad (3.3)$$

We will write the indices of λ in matrices when necessary, as in $\lambda \begin{pmatrix} 4 & 8 \\ 1 & 5 \end{pmatrix}$, which is the four-fermion channel that scatters two ingoing fermions in patches 1 and 5 to outgoing fermions in patches 4 and 8.

3.2 Renormalizing the full theory

Renormalizing these coupling *functions* means that we will compute their beta *functionals*, which give the change in the whole function as we change the probe scale. The beta functionals for v , g , V_F , and λ have been computed previously in [6]. The theoretical apparatus for the functional RG formalism is heavy, so we will not present it in full, but it is laid out in full in §V of [6]. We will motivate and discuss them here before focusing in on the most divergent and thus most interesting channel of the four-fermion interaction.

When we calculate vertex functions for this theory, we will obtain divergences, which must be canceled by the addition of counterterms to the action of Eq. 3.1. The beta functional of a particular coupling function will consist

of a few tree-level scaling term contributions that account for the scaling dimensions of the fields affected by that coupling and contributions from the counterterms that are computed from the divergent diagrams. We will first discuss the two main complications that arise when moving to *functional* renormalization from standard renormalization.

Fermi surface scaling. In relativistic quantum field theory, the scale transformation used when renormalizing from one energy scale to another is a simple dilatation: $k^\mu \mapsto e^{-\ell} k^\mu$. This is isotropic in four-momentum space because the theory is assumed to have Lorentz invariance, which makes this the only reasonable scale transformation to use.

In the presence of a Fermi surface we have a different story. The Fermi momentum k_F must be a part of the deep-IR description of the theory: for instance, the heat capacity of a Fermi liquid is proportional to the size of its Fermi surface, which is proportional to k_F in $2 + 1$ dimensions. This is clearly a probe of the system that is possible at arbitrarily low energy. The crucial difference from the relativistic case is that the zero-energy locus in momentum space isn't at $k^\mu = 0$: it's at $e(\vec{k}) = 0$ for the fermions and $\vec{q} = 0$ for the bosons. Because a gapless boson couples gapless fermions only when the fermions are at hot spots, we must take the hot spot to be the center of the scale transformation in each patch. Otherwise, we scale the x - and y -coordinates of the momentum \vec{k} equally, as they are considered the same by the boson propagator that will be responsible for most cutting off most loop integrals. Note that this scheme is very different from the relativistic one because \vec{k} is measured from the hot spot, not from the origin.

In the functional renormalization picture, this adds a complication: the momentum is not only an integration variable, but also a “continuous flavor” that is an argument of the coupling functions. This means that under an RG scaling transformation, the arguments of the functions transform. This generally means that we will be unable to find coupling functions that are truly fixed under RG flow. Instead, we will find that our coupling functions can be fixed when taking a rescaled momentum $K = ke^\ell$ as their argument (we will consistently use uppercase letters for rescaled momenta and lowercase for real momenta). This means that we will define our scale-dependent beta functionals as, for instance,

$$\beta_K^{(v)} = -\frac{\partial v_K(\ell)}{\partial \ell} - K \frac{\partial v_K(\ell)}{\partial K}. \quad (3.4)$$

We can still say that a set of couplings with scale-dependent beta functionals zero constitutes a fixed point: in a way reminiscent of the picture shown in Fig. 4 for the hot-spot theory, we broaden our definition of a fixed point in order to include the distinctly non-trivial phase that our system is in.

Extended minimal subtraction. In standard renormalization, we use a minimal subtraction scheme, in which the counterterms do not subtract the entire contribution from diagrams with UV divergences—they cancel out the divergences precisely, instead. When we allow full coupling functions, we open ourselves to the possibility of observable IR divergences stemming from integrations of couplings over momenta. This is important to consider for the four-fermion coupling λ . We must write counterterms not only for the obvious UV divergences, but also for the IR divergences that occur when we integrate the coupling functions over the phase space of their corresponding scattering processes—these types of quantum corrections are the source of our effective four-fermion term. We call this procedure the *extended minimal subtraction scheme*.

Adiabaticity. Our coupling function formalism is able to accommodate arbitrary sufficiently-smooth coupling functions, but it usually doesn’t have to. The couplings v , g , and V are marginal at tree level, so we don’t expect the momentum profiles that they acquire to be too dramatic. If their variance within a loop integral is sufficiently gradual, they won’t affect the degree to which it diverges. This is true for any quantum corrections that remain finite if we take the Fermi momentum k_F to infinity, such as the main contributions to the boson propagator and small-angle scattering. This essay will focus mostly on large-angle scatterings without adiabaticity, but it is important to make note of it because it shows the closeness of the theory of the full Fermi surface to the hot spot theory, which had no large-angle scattering—most of the calculations before λ will be the similar in both cases.

3.3 The non-Fermi liquid fixed point

Through similar calculations to those in Ch. 2.2, we can find the beta functionals for the full theory. These are governed by a set of crossovers in the momentum along the Fermi surface, shown in Fig. 5. Electrons with momenta greater than k_c are “cold,” meaning that even at the theory defined at

scale Λ , they do not receive contributions to their self-energy from the boson. Electrons with momentum less than k_h are “hot,” so they receive corrections all the way down to scale $\mu = \Lambda e^{-\ell}$. Electrons in between are “lukewarm,” so they were hot at scale Λ , but somewhere between Λ and μ were frozen out of interactions with the boson. This picture makes sense from the perspective of the scale transformation discussed in Chapter 3.2.

Because of the momentum-scaling transformation that comes with an energy-scaling renormalization transformation, it is impossible to find a fixed-point solution to the functional renormalization equations such that the coupling functions are truly invariant with the energy scale. However, similarly to how the hot-spot fixed point is best conceived in the perspective where g^2/v is considered to approach a fixed point even as g and v themselves go to zero, it is possible to solve for the coupling functions after first changing our coordinates, and thus our perspective on the problem. Once we shift to *rescaled momenta* $K = e^\ell k$ etc., it is possible to find fixed-point coupling functions up to smoothly varying crossovers.

As calculated in [6], the scale-dependent coupling functions, defined with argument K and for momentum crossovers $K_h = e^\ell k_h(\ell) = \frac{\Lambda}{4v_0(0)}$ and $K_c = e^\ell k_c(\ell) = \frac{\Lambda e^\ell}{4v_0(0)}$, are

$$v_K = v_0(0) \quad (3.5)$$

$$V_K = \begin{cases} 1 & |K| < K_h \\ \left(\frac{|K|}{K_h}\right)^{\alpha_1} & K_h < |K| < K_c \\ \left(\frac{K_c}{K_h}\right)^{\alpha_1} & K_c < |K| \end{cases} \quad (3.6)$$

$$g_K = \begin{cases} \sqrt{\pi v_0(0)/2} & |K| < K_h \\ \sqrt{\pi v_0(0)/2} \left(\frac{K_h}{|K|}\right)^{\alpha_0} & K_h < |K| < K_c \\ \left(\frac{K_h}{K_c}\right)^{\alpha_0} & K_c < |K| \end{cases} \quad (3.7)$$

$$g_{K,K'} = g_{\max(|K+K'|, c|K|, c|K'|)/2} \quad (3.8)$$

$$\alpha_1(\ell) = \frac{\sqrt{N_c^2 - 1}}{\sqrt{\ell_0 + \ell} \log(\ell_0 + \ell)} \quad (3.9)$$

$$\alpha_0(\ell) = \frac{1}{2\sqrt{N_c^2 - 1}\sqrt{\ell_0 + \ell}}. \quad (3.10)$$

It is also important to note the anomalous dimension of the fermions acquired

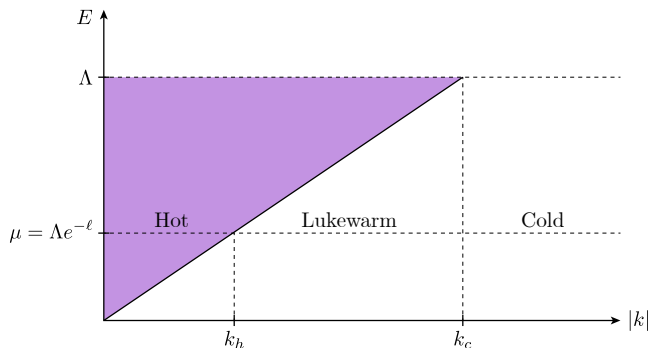


Figure 5: Here are the momentum crossovers used when defining the fixed point coupling functions. This figure is derived from Fig. 20 of [6].

through the interaction with the bosons: this is

$$\eta_K = \frac{(N_c^2 - 1)g_K^2}{2\pi^2 N_c c V_K} \frac{\Lambda}{\Lambda + 2cv_K |K|_\Lambda}, \quad (3.11)$$

where $|\cdot|_\Lambda$ is the smooth function $\sqrt{K^2 + \Lambda^2}$ that tends to $|K|$ in the limit of small $|\Lambda/K|$.

One interesting feature of this theory that becomes relevant for the four-fermion interaction is that when we work in rescaled momentum, the Fermi surface of the IR theory is in a sense no longer compact. This is because the physical momentum k_F that defines the size of a patch and of the Fermi surface is fixed under renormalization, meaning that its rescaled equivalent $K_F = k_F e^\ell$ must go to infinity. This concept is at the root of much of the odd behavior that we will see later in this essay.

4 The four-fermion coupling

Next we will look more closely at the four-fermion coupling. The quantum corrections and beta functional for all channels have been calculated in [6]. We will then go further, finding an expansion in v of the quasi-fixed-point four-fermion coupling.

Among the channels $\begin{pmatrix} N_1 & N_2 \\ N_3 & N_4 \end{pmatrix}$ of the four-fermion interaction, only some of them have IR divergences, and those that do split naturally into two groups, which we call Group 1 and Group 2, each of which are closed under renormalization flow. Group 1 only diverges for small-angle scatterings and

consists of $\{(\begin{smallmatrix} 1 & 1 \\ 1 & 1 \end{smallmatrix}), (\begin{smallmatrix} 1 & 4 \\ 1 & 4 \end{smallmatrix}), (\begin{smallmatrix} 1 & 4 \\ 4 & 1 \end{smallmatrix}), (\begin{smallmatrix} 4 & 4 \\ 4 & 4 \end{smallmatrix})\}$. These can be shown to diverge for momenta $(\begin{smallmatrix} k & 0 \\ 0 & k \end{smallmatrix})$ or $(\begin{smallmatrix} 0 & k \\ k & 0 \end{smallmatrix})$. There are four independent copies of Group 1 related by C_4 symmetry, and they do not mix with one another. Group 2 is $\{(\begin{smallmatrix} 1 & 5 \\ 1 & 5 \end{smallmatrix}), (\begin{smallmatrix} 4 & 8 \\ 4 & 8 \end{smallmatrix}), (\begin{smallmatrix} 1 & 5 \\ 4 & 8 \end{smallmatrix}), (\begin{smallmatrix} 4 & 8 \\ 1 & 5 \end{smallmatrix})\}$. The divergence of Group 2 is significantly more serious than Group 1, as is possible for pairs with zero center-of-mass momentum to scatter arbitrarily far from the hot spot to other such pairs while staying on the Fermi surface; these processes have momenta $(\begin{smallmatrix} p & -p \\ k & -k \end{smallmatrix})$. This two-dimensional space of IR divergence means that the $\lambda(\begin{smallmatrix} 1 & 5 \\ 1 & 5 \end{smallmatrix})$ process can impact fermions that we would have otherwise thought to be cold, that is, no longer under the influence of the spin fluctuations themselves. After computing λ^* , we will see the possible impact of this fact on the symmetries of the system in Chapter 5.

4.1 Quantum corrections and beta functionals

There are three types of processes that contribute to the four-fermion coupling λ : direct generation from spin fluctuations, linear mixing, and quadratic BCS processes. These are shown in Fig. 6. When performing an RG flow from a UV theory with $\lambda = 0$ in all channels, λ is initially only nonzero in the few channels that are directly generated by spin fluctuations, which are $(\begin{smallmatrix} M & N \\ M & N \end{smallmatrix})$. Immediately thereafter, additional channels acquire nonzero λ through linear mixing of the four-fermion process via the Yukawa interaction with an internal boson: these processes are linear in λ , so they are initially small, but they're very important to consider because many of the channels that they affect would otherwise be zero. The third type is quadratic in λ , and it describes the fusion of two four-fermion vertices; we call it the BCS term because of its similarities to the diagrams in the BCS theory of superconductivity. It takes a while to become important by virtue of its quadratic power.

The beta functional for the $\lambda(\begin{smallmatrix} 1 & 5 \\ 1 & 5 \end{smallmatrix})$ channel is computed in [6] to be, written

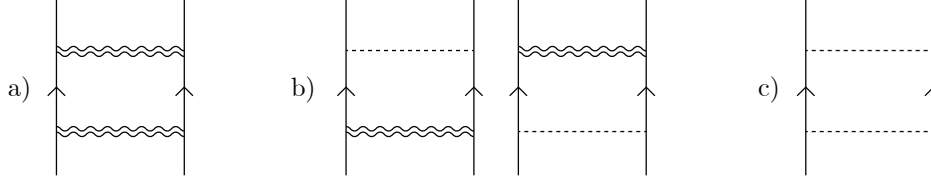


Figure 6: These are the four diagrams that contribute to the beta functional of $\lambda^{(\frac{1}{1} \frac{5}{5})}$. The dashed line is a four-fermion interaction and the double wiggly line is a fully-dressed boson propagator. Generation from spin fluctuations is (a), linear mixing is (b), and the BCS term is (c).

in rescaled momenta,

$$\begin{aligned}
\beta^{(\lambda);(\frac{1}{1} \frac{5}{5});\vec{\sigma}}_{\left(\begin{smallmatrix} P & -P \\ K & -K \end{smallmatrix}\right)} &= (1 + P\partial_P + K\partial_K + 2\eta_P + 2\eta_K)\lambda^{(\frac{1}{1} \frac{5}{5});\vec{\sigma}}_{\left(\begin{smallmatrix} P & -P \\ K & -K \end{smallmatrix}\right)} \\
&+ \int d\rho(Q) \left\{ \frac{1}{\pi} T_{\alpha\beta}^{\sigma_1\sigma_2} T_{\sigma_4\sigma_3}^{\alpha\beta} D_{\Lambda}(P;Q) D_{\Lambda}(Q;K) \right. \\
&- \frac{D_{\Lambda}(P;Q)}{2\pi} T_{\alpha\beta}^{\sigma_1\sigma_2} \lambda^{(\frac{4}{1} \frac{8}{5});\left(\begin{smallmatrix} \alpha & \beta \\ \sigma_4 & \sigma_3 \end{smallmatrix}\right)}_{\left(\begin{smallmatrix} Q & -Q \\ K & -K \end{smallmatrix}\right)} - \frac{D_{\Lambda}(Q;K)}{2\pi} \lambda^{(\frac{1}{4} \frac{5}{8});\left(\begin{smallmatrix} \sigma_1 & \sigma_2 \\ \alpha & \beta \end{smallmatrix}\right)}_{\left(\begin{smallmatrix} P & -P \\ Q & -Q \end{smallmatrix}\right)} T_{\sigma_4\sigma_3}^{\alpha\beta} \\
&\left. + \frac{1}{4\pi} \left(\lambda^{(\frac{1}{1} \frac{5}{5})}_{\left(\begin{smallmatrix} P & -P \\ Q & -Q \end{smallmatrix}\right)} \lambda^{(\frac{1}{1} \frac{5}{5})}_{\left(\begin{smallmatrix} Q & -Q \\ K & -K \end{smallmatrix}\right)} + \lambda^{(\frac{4}{1} \frac{8}{5})}_{\left(\begin{smallmatrix} P & -P \\ Q & -Q \end{smallmatrix}\right)} \lambda^{(\frac{4}{1} \frac{8}{5})}_{\left(\begin{smallmatrix} Q & -Q \\ K & -K \end{smallmatrix}\right)} \right) \right\}, \quad (4.1)
\end{aligned}$$

where we write

$$D_{\Lambda}(P, K) = \frac{g_{P,K}^2 \Lambda}{\Lambda + c(|P - Q|_{\Lambda} + |v_Q Q + v_P P|_{\Lambda})}, \quad d\rho(Q) = \frac{dQ}{2\pi \Lambda V_Q}$$

for the effective boson propagator and the phase space measure, respectively, and

$$T_{\sigma_4\sigma_3}^{\sigma_1\sigma_2} = \sum_{\alpha=1}^{N_c^2-1} \sigma_{\sigma_1\sigma_4}^{\alpha} \sigma_{\sigma_2\sigma_3}^{\alpha} = 2 \left(\delta_{\sigma_1\sigma_3} \delta_{\sigma_2\sigma_4} - \frac{1}{N_c} \delta_{\sigma_1\sigma_4} \delta_{\sigma_2\sigma_3} \right)$$

as the spin structure factor for the four-fermion interaction mediated by a boson. The three lines in the integral of Eq. 4.1 are the quantum corrections: the first one is from the spin fluctuations, the second is linear mixing, and the third is quadratic BCS terms. Very similar equations exist for the other

three channels of Group 2; we can put them all together by defining

$$\lambda = \begin{pmatrix} \lambda \begin{pmatrix} 1 & 5 \\ 1 & 5 \end{pmatrix} & \lambda \begin{pmatrix} 1 & 5 \\ 4 & 8 \end{pmatrix} \\ \lambda \begin{pmatrix} 4 & 8 \\ 1 & 5 \end{pmatrix} & \lambda \begin{pmatrix} 4 & 8 \\ 4 & 8 \end{pmatrix} \end{pmatrix}. \quad (4.2)$$

Another simplification can be made by eigendecomposing the spin structure tensor as $T_{\gamma\delta}^{\alpha\beta} = Y_+ S_{\gamma\delta}^{\alpha\beta} + Y_- A_{\gamma\delta}^{\alpha\beta}$, where $Y_{\pm} = \pm 2(1 \mp 1/N_c)$ are the eigenvalues and S and A project onto the eigenspaces. We will also normalize the couplings as $\lambda_{P,K} \mapsto \lambda_{P,K}/\sqrt{V_P V_K}$. All of this together, our beta functional is

$$\begin{aligned} \beta_{\begin{pmatrix} P & -P \\ K & -K \end{pmatrix}}^{(\lambda);\pm} &= (1 + P\partial_P + K\partial_K + 2\eta_P + 2\eta_K) \lambda_{\begin{pmatrix} P & -P \\ K & -K \end{pmatrix}}^{\pm} \\ &+ \frac{1}{4\pi} \int \frac{dQ}{2\pi\Lambda} \left[\lambda_{\begin{pmatrix} P & -P \\ Q & -Q \end{pmatrix}}^{\pm} - 2Y_{\pm} D_{\Lambda}(P; Q) \begin{pmatrix} 0 & 1 \\ 1 & 0 \end{pmatrix} \right] \\ &\times \left[\lambda_{\begin{pmatrix} Q & -Q \\ K & -K \end{pmatrix}}^{\pm} - 2Y_{\pm} D_{\Lambda}(Q; K) \begin{pmatrix} 0 & 1 \\ 1 & 0 \end{pmatrix} \right]. \end{aligned} \quad (4.3)$$

We can apply a similarity transform to λ such that the matrix $\begin{pmatrix} 0 & 1 \\ 1 & 0 \end{pmatrix}$ is diagonalized. We will index the channel by r , where $r = 1$ is the s -channel and $r = -1$ is the d -channel. With this convention, our final beta functional for λ is

$$\begin{aligned} \beta_{P,K}^{(\lambda);\pm,r} &= (1 + P\partial_P + K\partial_K + \eta_K + \eta_P) \lambda_{P,K}^{\pm,r} \\ &+ \int \frac{dQ}{2\pi\Lambda} \left[\lambda_{P,Q}^{\pm,r} - 2rY_{\pm} \frac{D_{\Lambda}(P; Q)}{\sqrt{V_P V_Q}} \right] \left[\lambda_{Q,K}^{\pm,r} - 2rY_{\pm} \frac{D_{\Lambda}(Q; K)}{\sqrt{V_Q V_K}} \right], \end{aligned} \quad (4.4)$$

where we have abbreviated $\begin{pmatrix} P & -P \\ K & -K \end{pmatrix} \rightarrow (P, K)$ in subscripts.

We want to find λ^* such that Eq. 4.4 is zero when acting on λ^* . This goal, however, has a serious problem. At a particular scale μ , the integral over Q should range from Λ to $\Lambda e^{\ell} = \Lambda^2/\mu$. But because $D_{\Lambda}(P, K) \sim v/c|K - P|$, it has the potential to diverge at high Q . This integral is first cut off by the bare boson kinetic term, which is present in the full theory but not in our effective theory in Eq. 3.1 at scale μ . Because our theory at scale μ requires information from the theory at scale $\Lambda > \mu$ in order to determine the flow of the couplings as μ is reduced, we seem to have encountered *UV/IR mixing*.

On first impression, this breaks the key assumption of effective field theories that the physics of different scales decouple from one another and that RG flows can always be computed from our theory without looking at any higher-energy behavior: this signals that something is wrong with either our theory or our description.

Thankfully, in this case the problem is with our description. If we define the *net two-body interaction* as

$$\tilde{\lambda}_{P,K}^{\pm,r} = \lambda_{P,K}^{\pm,r} - 2rY_{\pm} \frac{D_{\lambda}(P,K)}{\sqrt{V_P V_K}}, \quad (4.5)$$

we can see that its beta functional is

$$\beta_{P,K}^{(\tilde{\lambda});\pm,r} = (1 + P\partial_P + K\partial_K + \eta_K + \eta_P) \tilde{\lambda}_{P,K}^{\pm,r} + 2rY_{\pm} R(K, P) + \frac{1}{4\pi} \int \frac{dQ}{2\pi\Lambda} \tilde{\lambda}_{P,Q}^{\pm,r} \tilde{\lambda}_{Q,K}^{\pm,r}, \quad (4.6)$$

with

$$R(K, P) = \frac{g_{K,P}^2}{\sqrt{V_K V_P}} \frac{\Lambda^2}{(\Lambda + c|K - P| + c|v_K K + v_P P|)^2}.$$

Because there are no $\int \lambda D$ or $\int DD$ integrals, we have skirted the problem of needing to be cut off by the boson kinetic term, and the theory is free of UV/IR mixing when defined in terms of the net four-body interaction $\tilde{\lambda}$. One reason that this is a sensible way for an effective field theory to be is that there is no possible experiment that can measure λ alone in a theory at scale μ : everywhere that a four-fermion interaction can appear in a diagram, we could also have an internal boson with two Yukawa interactions. It therefore is very reasonable that the theory should be defined in terms of the net four-fermion interaction that takes both types of interaction into account. This is the quantity whose quasi-fixed-point value we will find in the next section.

4.2 The quasi-fixed point

Our next goal is to compute the function $\tilde{\lambda}^*$ that puts the right side of Eq. 4.6 to zero. Unfortunately, this is impossible: as shown in §VII-(c).2 of [6], for any finite value of v , there is no Hermitian coupling $\tilde{\lambda}^*$ whose beta function is zero. This is because the Fermi liquid is susceptible to the BCS instability, under which attractive four-fermion interactions are relevant and result in spontaneous symmetry breaking and a superconducting ground state. If at any point our $\tilde{\lambda}$ acquires a strongly attractive portion, the theory will flow

immediately to a superconducting phase. However, if $\tilde{\lambda}$ is not immediately attractive (as in the setting where the UV theory has $\lambda = 0$), the theory flows through a bottleneck region, where $\tilde{\lambda}$ flows very slowly because it is very close to true fixed point values of $\tilde{\lambda}$, but these values lie off of the real axis when $v \neq 0$, so a Hermitian theory will never actually get to them. We know that they must be close to the real axis because they are smoothly connected to the fixed point at $\lambda = 0, v = 0$ as a function of v , and v is small. Because the theory flows very slowly in this region, it is at essentially the same point in coupling space for a very long RG time. We refer to this as the *quasi-fixed point*, and the goal of this section is to find it by finding $\tilde{\lambda}^*$ as an expansion in v that sets Eq. 4.6 to zero.

The fixed-point equation is

$$0 = (1 + P\partial_P + K\partial_K + \eta_K + \eta_P)\tilde{\lambda}_{P,K}^* + 2rY_{\pm}R(P, K) + \frac{1}{4\pi} \int \frac{dQ}{2\pi\Lambda} \tilde{\lambda}_{P,Q}^* \tilde{\lambda}_{Q,K}^*. \quad (4.7)$$

The anomalous dimensions η are each of order vc^{-1} , so they are less important than $1 + P\partial_P + K\partial_K$ at low order. The inhomogeneous source term R is of order vc^{-1} . These facts imply the possibility of an expansion in small v that decomposes $\tilde{\lambda}^*$ into terms at different orders in v . Because we are specifically interested in large-angle scattering, we will also pay attention to their orders in $|P - K|$. Between v , c , $1/\log v$, and $1/|P - K|$, there are many small parameters to keep track of. In light of this, we will number our contributions from the BCS term as $\tilde{\lambda}_i$ sequentially with i , but each $\tilde{\lambda}$ may end up having several subterms at different orders in v and $1/|P - K|$. We will also call by $\tilde{\lambda}_i$ the terms generated by the source term $\eta\tilde{\lambda}_i$. The different contributions of different origins are difficult to keep track of, but the final result ordered by magnitude in v and $1/|P - K|$ can be seen in Eq. 4.26.

Assuming that the BCS term is higher-order than R , we can find the first-order approximation

$$0 = (1 + P\partial_P + K\partial_K)\tilde{\lambda}_0 + 2rY_{\pm}R. \quad (4.8)$$

This is solved by

$$\tilde{\lambda}_0(P, K) = -2rY_{\pm}D_{\Lambda}(P, K) = -\frac{\pi rY_{\pm}v\Lambda}{\Lambda + c|P - K|_{\Lambda} + cv|P + K|_{\Lambda}}, \quad (4.9)$$

where we used $g_{P,K}^2 \approx \pi v/2$. When the momenta are larger than Λ , this is of order vc^{-1} . Note that this is also the bare value of $\tilde{\lambda}$, because $\tilde{\lambda} = \lambda - 2rY_{\pm}D$

and $\lambda = 0$ in the UV theory. This alleviates any concerns about homogeneous solutions to Eq. 4.8 by serving as a boundary condition for the RG equation Eq. 4.6.

Now we can compute the BCS term to justify our assumption that is smaller than $\tilde{\lambda}_0$. We notate it as

$$I_{00} \equiv \frac{1}{4\pi} \int \frac{dQ}{2\pi\Lambda} \tilde{\lambda}_0(P, Q) \tilde{\lambda}_0(Q, K) \quad (4.10)$$

$$= -\frac{Y_{\pm}^2 \Lambda v^2 \log v}{2c^2 |P - K|}, \quad (4.11)$$

which is valid up to order $|P - K|^{-1}$ and $v^3 \log v$, focusing again on large-angle scattering. We will see very directly in Chapter 5 that the biggest difference between this fixed point and the Fermi liquid is through these terms of order $|P - K|^{-1}$, so we will neglect all others. We can manipulate the definition $c = \sqrt{v \log(1/v)}/4$ to see that $\log v = -16c^2/v$, so this expression is

$$I_{00} = \frac{8Y_{\pm}^2 \Lambda v}{|P - K|}. \quad (4.12)$$

This is of order v , which is still smaller than $\tilde{\lambda}_0$ and R , which are order vc^{-1} , so we have enough suppression to suggest that this is a reasonable expansion.

Next, we take I_{00} as a new source term to get the term $\tilde{\lambda}_1$. The equation that this must satisfy is

$$0 = (1 + P\partial_P + K\partial_K) \tilde{\lambda}_1 + I_{00}, \quad (4.13)$$

which is solved by

$$\tilde{\lambda}_1 = -\frac{8Y_{\pm}^2 \Lambda v \log |P - K|}{|P - K|}. \quad (4.14)$$

This $\tilde{\lambda}_1$ has an enhancement at large angle when compared to the bare interaction $\tilde{\lambda}_0$, and it is of the same sign. This means that the BCS term at lowest order is pushing the fixed-point coupling to be even more strongly attracting than it was originally.

Next we'll compute the first two corrections from the anomalous dimension η , which we'll write as $\tilde{\lambda}_{0'}$ and $\tilde{\lambda}_{1'}$. These are defined as solutions to the equation

$$0 = (1 + K\partial_K + P\partial_P) \tilde{\lambda}_{i'} + \eta \tilde{\lambda}_i, \quad (4.15)$$

where $\eta \equiv \eta_K + \eta_P$. The correction from $\tilde{\lambda}_0$ is

$$\tilde{\lambda}_{0'} = \frac{3Y_{\pm}r\Lambda v^2 \log(c|P-K|)}{4c^2|P-K|}. \quad (4.16)$$

However, we also know that $\log c = -2 \log 2 + \frac{1}{2} \log v + \frac{1}{2} \log \log \frac{1}{v} \approx -8c^2/v$ from the definition of c . This means that our actual correction is

$$\tilde{\lambda}_{0'} = -\frac{6Y_{\pm}r\Lambda v}{|P-K|} + \frac{3Y_{\pm}r\Lambda v^2 \log|P-K|}{4c^2|P-K|}. \quad (4.17)$$

This means that it will contribute even more strongly to the BCS term. Note that the first term of this expression modifies $\tilde{\lambda}_0$, which is order v/c , by something at order v , so there is suppression by $c \sim v^{1/2} \log^{1/2} v$; and the second term modifies $\tilde{\lambda}_1$, which is order v , by something at v^2/c^2 , so the suppression is by $v/c^2 \sim 1/\log(v)$. This means that considering the terms generated when we take $\eta\tilde{\lambda}_{0'}$ itself as a source will be suppressed by additional factors of c , and we don't expect them to be important. Next we can compute the term generated by $\eta\tilde{\lambda}_1$ to be

$$\tilde{\lambda}_{1'} = \frac{3Y_{\pm}^2\Lambda v^2 \log^2|P-K|}{\pi c|P-K|} - \frac{6Y_{\pm}^2v^3|P+K| \log|P-K|}{\pi|P-K|}. \quad (4.18)$$

The first term is new and important as the first $\log^2|P-K|$ correction, and the second is dominated by its equivalent at order v^2/c^2 from $\tilde{\lambda}_{0'}$ and at v from $\tilde{\lambda}_1$. For these to be surmounted, we would need $v^3|P+K| \gtrsim v$, which we can assume to not be true.

Because the BCS integrand is $\tilde{\lambda}\tilde{\lambda}$, we have terms for every pair of $\tilde{\lambda}_i$ in our expansion. Next we compute them for our new terms:

$$I_{01} = \frac{1}{4\pi} \int \frac{dQ}{2\pi\Lambda} \tilde{\lambda}_0(P, Q) \tilde{\lambda}_1(Q, K) \quad (4.19)$$

$$\begin{aligned} &= \frac{1}{4\pi} \int \frac{dQ}{2\pi\Lambda} \left(-\frac{\pi v r Y_{\pm} \Lambda}{\Lambda + |P-Q| + c v |P+Q|} \right) \left(\frac{8Y_{\pm}^2 \Lambda v \log|Q-K|}{|Q-K|} \right) \\ &= \frac{\Lambda v^2 Y_{\pm}^3 r (\pi^2 - 2 \log^2|P-K| - 2 \log(c|P-K|))}{\pi c |P-K|} \end{aligned} \quad (4.20)$$

$$= \frac{\pi Y_{\pm}^3 r \Lambda v^2}{c |P-K|} + \frac{16 Y_{\pm}^3 r \Lambda c v \log|P-K|}{\pi |P-K|} - \frac{2 Y_{\pm}^3 r \Lambda v^2 \log^2|P-K|}{c \pi |P-K|}, \quad (4.21)$$

where we've used $\log c \approx -8c^2/v$. This term occurs in the fixed-point equation twice, as $I_{01} + I_{10} = 2I_{01}$. The terms that it generates are

$$0 = (1 + K\partial_K + P\partial_P)\tilde{\lambda}_2 + 2I_{01} \quad (4.22)$$

$$\tilde{\lambda}_2 = -\frac{2\pi Y_{\pm}^3 r \Lambda v^2 \log |P - K|}{c|P - K|} - \frac{16Y_{\pm}^3 r \Lambda c v \log^2 |P - K|}{\pi|P - K|} + \frac{4Y_{\pm}^3 r \Lambda v^2 \log^3 |P - K|}{3\pi c|P - K|}. \quad (4.23)$$

We can write the total $\tilde{\lambda}^*$ that we've computed so far, expressed as a function of $Q = |P - K|$, as

$$\tilde{\lambda}^*(Q) = \frac{1}{Q}(-\pi Y_{\pm} r \Lambda v/c - 6Y_{\pm} r \Lambda v) \quad (4.24)$$

$$+ \frac{\log Q}{Q}(-Y_{\pm}^2 \Lambda v + 3Y_{\pm} r \Lambda v^2/4c^2 - 2\pi Y_{\pm}^3 r \Lambda v^2/c) \quad (4.25)$$

$$+ \frac{\log^2 Q}{Q}(3Y_{\pm}^2 \Lambda v^2/\pi c - 16Y_{\pm}^3 r \Lambda c v/\pi), \quad (4.26)$$

where we have neglected dependence on $|P + K|/|P - K|$ and $\log^3 |P - K|$. Each of these will pick up further corrections as we continue computing terms, but as we have seen, they steadily become less important by factors of c . In our analysis of the symmetry group respected by this fixed-point coupling, we will see that the last term in each of the lines of 4.26 are not relevant to our computation, and we can expect even further suppression as we go.

5 IR symmetry group

In this chapter, we wish to examine the differences in the IR symmetry group of the Fermi liquid and that of our model. Our goal is to see if the symmetries are the same, or if the non-Fermi liquid fails to support an emergent symmetry group that is equivalent to that of the Fermi liquid.

5.1 Ersatz Fermi liquids

Defining a Fermi liquid by its dispersion $e(\vec{k})$, the only operators that exist in a theory at scale μ are ψ_k^\dagger and ψ_k such that $|e(\vec{k})| < \mu$. In the deep IR, the only operators in the theory are those that are actually on the Fermi

surface, so they have \vec{k} such that $e(\vec{k}) = 0$. In our (2+1)-dimensional setting, the Fermi surface is a one-dimensional submanifold of the Brillouin zone. Because large-angle scattering is irrelevant for a Fermi liquid, the action of the IR theory is an integral over quadratic terms $\psi_k^\dagger \psi_k$, with k taking values on or very close to the Fermi surface. In a finite-size system with an IR cutoff, momentum space is discretized and we can conceive of these number operators as N free fermions, each of which has its own independent $U(1)$ symmetry. Taking this cutoff to infinity, the symmetry group is $LU(1)$, the “loop group” of $U(1)$, whose elements are maps $\psi_k \mapsto e^{i\theta_k} \psi_k$, where θ_k is a continuous function from an S^1 as the Fermi surface to an S^1 as the phases $[0, 2\pi)$.

This picture is very straightforward for the Fermi liquid because its theory is simple to do calculations with, and it is straightforward to compute the change in the theory under an action of $LU(1)$ and show that it vanishes as the energy scale goes to zero. In [7], this result was generalized: it was proven that for a clean, lattice system in a phase that is *compressible*—meaning that it is possible for it to exist at a continuously tunable filling ν defined as the number of electrons per lattice cell—it is impossible for that system to have a symmetry group that is a compact Lie group. It must have a symmetry group that is in a sense larger; they name the class of metals that share $LU(1)$ symmetry and other kinematic properties with Fermi liquids as *ersatz Fermi liquids*.

They then conjecture that all non-Fermi liquid behavior arises from ersatz Fermi liquids, where all of the observed differences are purely dynamical, not kinematic. The group $LU(1)$ isn’t quite applicable to our system, because we know that in the IR, the Yukawa interaction couples hot spots N and \bar{N} and the effective four-fermion interaction couples the hot spots N and $(N + 4) \bmod 8$. Another way to think of this is that $LU(1)$ is appropriate for a system that preserves the fermion density operator $\rho_{N,k} = \psi_{N,k}^\dagger \psi_{N,k}$, but ours only preserves a modified operator $\tilde{\rho}_{N,k} = \rho_{N,k} + \rho_{\bar{N},k} + \rho_{N+4,-k} + \rho_{\bar{N}+4,-k}$. The natural extension of $LU(1)$ to our system is thus the arbitrary functions θ_k on patch 1, with patches 4, 5, and 8 phase-shifted correspondingly. This differs from $LU(1)$ in that the domain space is no longer compact, but it is similar in spirit. We want to see if this symmetry emerges in the IR as $LU(1)$ emerges in the IR theory of a regular Fermi liquid. The emergence of this other group, which we call $PU(1)$ for patch- $U(1)$, is an equivalent conjecture to that in [7]. Finding that our system does not have this emergent symmetry would constitute a counterexample.

5.2 Emergent symmetry (or lack thereof)

Under the action of PU(1) defined by a function θ_k , the kinetic and Yukawa terms of our action in Eq. 3.1 are unchanged, for the same reason that the kinetic term is unchanged for a Fermi liquid. The rescaled four-fermion term in the $(\frac{1}{2} \frac{5}{2})$ channel with momenta $(\frac{P}{K} \frac{-P}{-K})$ changes as

$$S' = \int \frac{dK dP}{4\Lambda} \tilde{\lambda}^*(K, P) e^{i(\theta_P + \theta_{-P} - \theta_K - \theta_{-K})} \psi_K^\dagger \psi_{-K}^\dagger \psi_{-P} \psi_P, \quad (5.1)$$

where we have already integrated over the other momenta, using up the delta function and implicitly keeping us on the manifold of external momenta for which $\tilde{\lambda}^*$ has an IR divergence. This is certainly unchanged from the original action for θ that is an odd function of K , so we project out its odd part and only consider even θ . Taking the functional derivative for small θ , this becomes

$$\delta S = 2i \int \frac{dK dP}{4\Lambda} \tilde{\lambda}^*(K, P) (\theta_P - \theta_K) \psi_K^\dagger \psi_{-K}^\dagger \psi_{-P} \psi_P. \quad (5.2)$$

Now we consider the functional form of θ and the bounds of integration. The key question of this essay is if there exists some function θ such that

$$\lim_{\ell \rightarrow \infty} \frac{\delta S[\theta]}{S_0} \neq 0, \quad (5.3)$$

where the limit $\ell \rightarrow \infty$ is the same as $\mu \rightarrow 0$, and S_0 is the kinetic term $\int dK \psi_K^\dagger \psi_K$. This is necessary because the kinetic term itself goes as K_F , but we know it to be marginal.

The group PU(1) requires smoothness, so it does not include step functions: these are not even symmetries of Fermi liquids because they result in a change to the action when perturbed by irrelevant four-fermion terms. Our expression computed in Section 4.2 is specifically valid for large $|P - K|$ and small $|P + K|$, so we pick a θ_K that is a bump function around $K = 0$ with width $2K^*$. We are expressing these here in rescaled momenta, but we will need this to be defined as a constant in physical momentum space, so this will transform as $K^* = k^* e^\ell$ under an RG transformation. With this function θ , our integration bounds are

$$\delta S = 4i \int_{K_*}^{K_F} dK \int_{-K_F}^{-K^*} \frac{dP}{4\Lambda} \tilde{\lambda}^*(K, P) \psi_K^\dagger \psi_{-K}^\dagger \psi_{-P} \psi_P. \quad (5.4)$$

Shifting our coordinate to $Q = |P - K|$, this is

$$\delta S = 4i \int_{K_*}^{K_F} dK \int_{K_*+K}^{K_F+K} \frac{dQ}{4\Lambda} \tilde{\lambda}^*(K, K+Q) \psi_K^\dagger \psi_{-K}^\dagger \psi_{-K-Q} \psi_{K+Q}. \quad (5.5)$$

Now we need to deal with the fields ψ^\dagger and ψ . If there exists any low-energy state for which there exists any element of $\text{PU}(1)$ that is not a symmetry, the $\text{PU}(1)$ is not emergent—here a low-energy state is a member of the Hilbert space spanned by states with energy density less than μ^2 . We know that the ground state of our theory is a BCS superconductor, for which $\psi_K^\dagger \psi_{-K}^\dagger \psi_{-K-Q} \psi_{K+Q}$ has a very weak dependence on Q over its whole range. Because of the existence of this state in the Hilbert space, we can safely neglect the fields in the regime that we are considering.

We also want to account for the S_0 in Eq. 5.3. The integral $\int_{K_*}^{K_F} dK$ is the same as that of the kinetic term, and we expect it to diverge like K_F in the large- ℓ limit. Our integral of interest is therefore

$$\frac{\delta S}{S_0} \sim \int_{K_*}^{K_F} \frac{dQ}{\Lambda} \tilde{\lambda}^*(0, Q). \quad (5.6)$$

The lowest-order form of $\tilde{\lambda}^*$ is $\tilde{\lambda}_0$, which is like $|Q|^{-1}$ at large Q . We can consider the higher-order corrections to $\tilde{\lambda}^*$ as altering the *exponent* of this expression, using the expansion

$$\left| \frac{1}{Q} \right|^{1+\alpha} = \frac{1}{|Q|} - \frac{\alpha \log |Q|}{|Q|} + \frac{\alpha^2 \log^2 |Q|}{2|Q|} + \dots \quad (5.7)$$

We are thus principally concerned with the terms $(\log^n |Q|)/|Q|$ that we found in our expansion for $\tilde{\lambda}^*$ in Eq. 4.26. We will take $N_c = 2$ in the $(s, +)$ channel, so $Y_+ = 1$ and $r = 1$. Factoring out the coefficient of $\tilde{\lambda}_0$ gives

$$\tilde{\lambda}^* = -\frac{\pi v \Lambda}{c} \left(\frac{1}{Q} + \frac{\log Q}{Q} (8c/\pi - 3v/4\pi c + 2v) + \frac{\log^2 Q}{2Q} (-6v/\pi^2 + 32c^2/\pi^2) \right). \quad (5.8)$$

The coefficient of the $\log Q/Q$ term of the expansion determines α , which tells us that

$$\alpha = -\frac{8c}{\pi} + \frac{3v}{4c} - 2\pi v. \quad (5.9)$$

For small v , this is very close to zero and the first two terms have similar magnitude but opposite sign. However, the first one wins out, and the exponent is negative for all $v \lesssim 0.81$, which certainly includes the regime that we're interested in. As v goes to zero, the dominant term is $-8c/\pi$. The dominant piece of the $\log^2 Q/Q$ term is $16c^2/\pi^2$, which is a factor of two away from being $\alpha^2/2$ as desired. We expect that the factor of two can be traced back by treating the relative magnitudes of v and $\log(1/v)$ more carefully.

After factoring out the coefficients from $\tilde{\lambda}_0$, our full integral is

$$\frac{\delta S}{S_0} \sim -\frac{\pi v \Lambda}{c} \int_{K^*}^{K_F} \frac{dQ}{\Lambda} \left(\frac{1}{Q} \right)^{1+\alpha} \quad (5.10)$$

$$= -\frac{\pi v}{c\alpha} \left[(K^*)^{-\alpha} - (K_F)^{-\alpha} \right] \quad (5.11)$$

$$= -\frac{\pi v}{c\alpha} \left[(k^*)^{-\alpha} - (k_F)^{-\alpha} \right] e^{-\alpha\ell} \quad (5.12)$$

$$\approx -\frac{\pi v e^{-\alpha\ell}}{c} \log \left(\frac{k_F}{k^*} \right). \quad (5.13)$$

The last approximation is valid for small α . When we take the limit as ℓ goes to infinity, this expression diverges for negative α and goes to zero for positive α (it also diverges logarithmically for $\alpha = 0$). Because we know that $\alpha < 0$ from Eq. 5.9, we have shown that this element of $\text{PU}(1)$ is not an emergent symmetry of our low-energy theory.

6 Discussion

Non-Fermi liquids are generally difficult to solve, and we are still very far from understanding the full space of metallic systems that nature allows. Using the theory of [1–3, 6] that is solvable in the limit of small nesting angle, we are able to study the ways in which non-Fermi liquids are able to diverge from the far better-understood Fermi liquid theory. In this work, we have shown that this theory does not have the same emergent symmetry group as a Fermi liquid would, which provides a counterexample to a conjecture of [7].

We still have very little information about the full IR emergent symmetry group of our theory. The main theorem of [7] shows that it must be larger than any compact Lie group, and we have shown that it is not the group $\text{PU}(1)$ that would emerge if it were an ersatz Fermi liquid by finding one element of $\text{PU}(1)$ that is not a symmetry. A deeper understanding of the

symmetry group that actually emerges requires that we know the functional form of $\tilde{\lambda}^*$ in more detail: if our expansion were to also include the dependence on $|P + K|$, which is not leading-order when compared to $|P - K|$, we could rule out much larger subsets of $\text{PU}(1)$ than just that considered in Chapter 5.

It is also worthwhile to study the effects of higher-fermion interactions on the emergent symmetry group. The six-fermion interaction is probably irrelevant for the purpose of vertex functions, as argued in [6]. However, we expect that it and other higher-fermion interactions could still impact the low-energy symmetry group by explicitly breaking specific elements as we have shown to occur for the four-fermion interaction, but also possibly by putting bounds on the smoothness of θ_k , which would be a substantial, qualitative change to the symmetry.

7 Acknowledgements

Thank you to my wonderful advisor, Sung-Sik Lee, for proposing this fascinating project, for his endless enthusiasm for physics, and for always making me feel better coming out of meetings than I did going into them. Thank you to Francisco Borges for guiding me through his paper and always making time to answer my simple questions. Thank you to Leonardo Lessa for his helpful comments on an early draft of this essay.

Thank you to my friends: thank you to Dawit Belayneh, for the jazz, the hexagons, the ቆሎ and ቊኮ, and for showing me what it means to be a good friend. Harika arkadaşlığı için, Türkçe hocamla kazların padişahı olan Sercan Hüsnügil'e teşekkürler ederim. Thank you to Cole Coughlin, who opened my eyes to whole new way to practice and experience physics and never let conventional wisdom get in the way of what is true and right. Le agradezco a Raquel Izquierdo García, que me enseñó mucho de poesía, de física, de español, y de amistad. Thank you to James Munday, for always doing asymptotic analysis when we needed it, for accompanying me on runs for tasty little treats, for being an excellent squash partner, and for his friendship. Thank you to these people and the rest of my PSI class for all that they have shared with me and allowed me to share with them this year, about physics and life and everything else. I will miss them all so much, and I am so much looking forward to visiting them all in Canada and beyond in the next few years.

Thank you to my family, whose support has always allowed me to follow my dreams. And thank you to Zoë Marschner, for coming all the way to Waterloo to visit me despite the geese and the cold, for making the lovely figures in this essay, for Lech the tardigrade, for all of our past and future hikes and road trips and high points, and for her love.

References

- [1] A. Schlief, P. Lunts, and S.-S. Lee, “Exact critical exponents for the antiferromagnetic quantum critical metal in two dimensions,” *Physical Review X* **7** no. 2, (2017) 021010.
- [2] S. Sur and S.-S. Lee, “Quasilocal strange metal,” *Physical Review B* **91** no. 12, (2015) 125136.
- [3] P. Lunts, A. Schlief, and S.-S. Lee, “Emergence of a control parameter for the antiferromagnetic quantum critical metal,” *Physical Review B* **95** no. 24, (2017) 245109.
- [4] S. Sachdev, *Quantum Phase Transitions*. Cambridge University Press, 2011.
- [5] R. Shankar, “Renormalization-group approach to interacting fermions,” *Reviews of Modern Physics* **66** no. 1, (1994) 129.
- [6] F. Borges, A. Borissov, A. Singh, A. Schlief, and S.-S. Lee, “Field-theoretic functional renormalization group formalism for non-fermi liquids and its application to the antiferromagnetic quantum critical metal in two dimensions,” *Annals of Physics* **450** (Mar, 2023) 169221. <https://doi.org/10.1016%2Fj.aop.2023.169221>.
- [7] D. V. Else, R. Thorngren, and T. Senthil, “Non-fermi liquids as ersatz fermi liquids: general constraints on compressible metals,” *Physical Review X* **11** no. 2, (2021) 021005.
- [8] L. Landau, “On the theory of the fermi liquid,” *Sov. Phys. JETP* **8** no. 1, (1959) 70.
- [9] K. Wilson, “Collective properties of physical systems,” in *Nobel Symposium*, vol. 24, p. 68. 1974.

- [10] S.-S. Lee, “Recent developments in non-fermi liquid theory,” *Annual Review of Condensed Matter Physics* **9** (2018) 227–244.
- [11] A. Kitaev, V. Lebedev, and M. Feigel’man, “Periodic table for topological insulators and superconductors,” in *AIP Conference Proceedings*. AIP, 2009. <https://doi.org/10.1063%2F1.3149495>.
- [12] B. Zeng, X. Chen, D.-L. Zhou, and X.-G. Wen, *Quantum information meets quantum matter*. Springer, 2019.
- [13] X.-G. Wen, “Classification of gapped quantum liquid phases of matter,” *Topological Phases of Matter and Quantum Computation* **747** (2020) 165.
- [14] A. Schliefl, P. Lunts, and S.-S. Lee, “Noncommutativity between the low-energy limit and integer dimension limits in the ε expansion: A case study of the antiferromagnetic quantum critical metal,” *Physical Review B* **98** no. 7, (2018) 075140.
- [15] S. Sur and S.-S. Lee, “Chiral non-fermi liquids,” *Physical Review B* **90** no. 4, (2014) 045121.